

A new ellipse fitting method of the minimum differential-mode noise in the atom interference gravimeter

Aopeng Xu(许翱鹏), Zhaoying Wang(王兆英), Delong Kong(孔德龙), Zhijie Fu(付志杰), Qiang Lin(林强)

Citation: Chin. Phys. B . 2018, 27(7): 070203. **doi:** 10.1088/1674-1056/27/7/070203

Journal homepage: http://cpb.iphy.ac.cn; http://iopscience.iop.org/cpb

What follows is a list of articles you may be interested in

Multi-window transparency and fast-slow light switching in a quadratically coupled optomechanical system assisted with three-level atoms

Wan-Ying Wei(魏晚迎), Ya-Fei Yu(於亚飞), Zhi-Ming Zhang(张智明)

Chin. Phys. B . 2018, 27(3): 034204. **doi:** 10.1088/1674-1056/27/3/034204

Parallel generation of 31 tripartite entangled states based on optical frequency combs

Jing Zhang(张静), Yan-Fang Wang(王艳芳), Xiao-Yu Liu(刘晓宇), Rong-Guo Yang(杨荣国)

Chin. Phys. B . 2017, 26(12): 124205. **doi:** 10.1088/1674-1056/26/12/124205

Generation of squeezed vacuum on cesium D2 line down to kilohertz range

Jian-Feng Tian(田剑锋), Guan-Hua Zuo(左冠华), Yu-Chi Zhang(张玉驰), Gang Li(李刚), Peng-Fei Zhang(张鹏飞), Tian-Cai Zhang(张天才)

Chin. Phys. B . 2017, 26(12): 124206. **doi:** 10.1088/1674-1056/26/12/124206

Super-resolution and super-sensitivity of entangled squeezed vacuum state using optimal detection strategy

Jiandong Zhang(张建东), Zijing Zhang(张子静), Longzhu Cen(岑龙柱), Shuo Li(李硕), Yuan Zhao(赵远), Feng Wang(王峰)

Chin. Phys. B . 2017, 26(9): 094204. **doi:** 10.1088/1674-1056/26/9/094204

A scheme for Sagnac-effect quantum enhancement with Fock state light input

Kun Chen(陈坤), Shu-Xin Chen(陈树新), De-Wei Wu(吴德伟), Chun-Yan Yang(杨春燕), Qiang Miao(苗强)

Chin. Phys. B . 2017, 26(9): 094212. **doi:** 10.1088/1674-1056/26/9/094212

A new ellipse fitting method of the minimum differential-mode noise in the atom interference gravimeter*

Aopeng Xu(许翱鹏)[1], Zhaoying Wang(王兆英)[1,†], Delong Kong(孔德龙)[1], Zhijie Fu(付志杰)[1], and Qiang Lin(林强)[2]

[1] *Institute of Optics, Department of Physics, Zhejiang University, Hangzhou* 310027, *China*
[2] *Center for Optics and Optoelectronics Research, College of Science, Zhejiang University of Technology, Hangzhou* 310023, *China*

(Received 5 February 2018; revised manuscript received 3 May 2018; published online 25 June 2018)

Ellipse fitting is a useful tool to obtain the differential signal of two atom interference gravimeters. The quality standard of ellipse fitting should be the deviation between the true phase and the fitting phase of the interference fringe. In this paper, we present a new algorithm to fit the ellipse. The algorithm is to minimize the differential noise of two interference gravimeters and obtain a more accurate value of the gravity gradient. We have theoretically derived the expression of the differential-mode noise and implemented the ellipse fitting in the program. This new algorithm is also compared with the classical methods.

Keywords: ellipse fitting, atom interference, gravity measurement

PACS: 02.60.Ed, 42.50.–p **DOI:** 10.1088/1674-1056/27/7/070203

1. Introduction

The measurement of the gravity field is very important. The average gravitational field near the Earth can be used to assess the effect of the Earth's gravitational equivalent and other forces, to reflect the different levels of the Earth's interior details.[1–3] In the field of fundamental physics, gravity measurement can be used for Kibble balance, measurement of the gravitational constant, and tests of general relativity.[4–8]

The cold atom gravimeter was introduced more than twenty years ago, and became a useful tool to measure the gravity.[9,10] An atom gradio-gravimeter was presented by using two sets of cold atom gravimeters working simultaneously and sharing a Raman beam. A significant noise of the cold atom gradio-gravimeter is the common mode noise, such as the vibration of the retro-reflection mirror, and the phase noise of the Raman beam.[11–13] In order to restrain the common mode noise, one can form the Lissajous figure by combining the two interference fringes. Usually this Lissajous figure has an ellipse shape.

Ellipse fitting is a useful tool to obtain the differential signal of two atom interference gravimeters, which has been present in many papers.[14–16] There are some classical algorithms of ellipse fitting, such as algebraic fit and geometric fit.[17–20] Determining the parameters of the minimized algebraic distance in the least squares sense will be denoted by algebraic fit, for which the sum of the squared distance from the data points to the ellipse is minimal will be referred to as the geometric fit.

The algebraic fit is widely used in phase extraction between two atom interference gravimeters.[14,16] However, algebraic fitting is more sensitive to outlying points outside of the ellipse than to outlying points inside the ellipse. The algebraic fit will be biased away from the appropriate phase value if the data points are noisy. Using the geometric fit may reduce the sensitivity, and the bias between the appropriate phase and the fitting phase can be smaller.[14]

The geometric fit is minimizing the squared geometric distance to each point. The geometric distance could not be shown as an explicit expression, and the geometric fit will consume a lot of computing resources. Gander introduced a modification to the algebraic fit of an ellipse in 1994. The algorithm weights the points such that the algebraic solution comes closer to the geometric solution.[17]

The geometric fit is considered as the best fit in many areas, such as computer graphics, coordinate meteorology, statistics, etc. In the application of the atom interferometer, both algebraic distance and geometric distance do not have a physical meaning. Therefore, we cannot consider the geometric fit as the best fit.

In this paper, we present a new algorithm to fit the ellipse. The aim of the fitting is minimizing the differential-mode noise of two interference gravimeters. Meanwhile, we compared the fitting result of our new algorithm with the algebraic fit and geometric fit.

2. Theory

2.1. Phase difference between two atom interferometers

The principle of the cold atom gravimeter has been well described in many works. The model of a basic Mach–

*Project supported by the National Key Research and Development Program of China (Grant No. 2017YFC0601602) and the Fundamental Research Funds for the Central Universities, China (Grant Nos. 2017FZA3005 and 2018FZA3005).

†Corresponding author. E-mail: zhaoyingwang@zju.edu.cn

© 2018 Chinese Physical Society and IOP Publishing Ltd

Zehnder type atom interferometer and the stimulated Raman transitions were described in some papers.[21] Our experimental apparatus of the atom gravimeter has been described in detail in a previous paper.[22] To measure the gravity gradient, two sets of gravimeters are installed vertically, working synchronously and sharing the same Raman beams. The stimulated Raman transitions manipulate the atom population of the two ground hyperfine sublevels $^5S_{1/2}$, $F=1$ and $^5S_{1/2}$, $F=2$ of the cooled ^{87}Rb atoms. Through a sequence of three Raman laser pulses $\pi/2$–π–$\pi/2$, the atomic wave packets would be split, redirected, and recombined. When the state of the atoms changes during the interaction with the Raman beams, there would be an additional phase imprinted onto the atoms by the Raman beams. Assuming all of the ^{87}Rb atoms are in the initial state of $F=2$, at the end of the interferometer, the interference fringes can be observed and the atom probability in the $F=1$ state is given by[23]

$$P_{2\to1}=\frac{1}{2}[1-\cos(\boldsymbol{k}_{\text{eff}}\cdot\boldsymbol{g}-\alpha)T^2+\phi_0], \tag{1}$$

where $\boldsymbol{k}_{\text{eff}}=\boldsymbol{k}_1-\boldsymbol{k}_2$ is the effective wave vector of the Raman beams, T is the time interval between two neighboring Raman pulses, and α is the chirp rate of the effective Raman laser frequency used to compensate the Doppler shift due to gravity $\boldsymbol{g}$.

The interference fringes of the gravimeter are sinusoidal. The two sinusoidal signals can be written as

$$P_x=A_x+B_x\cos\phi_x, \tag{2}$$

$$P_y=A_y+B_y\cos\phi_y=A_y+B_y\cos(\phi_x+\Delta\phi), \tag{3}$$

where A_x and A_y are the offsets of the sinusoidal signals, B_x and B_y are the amplitudes, ϕ_x and ϕ_y are the phases of the interferometers, and $\Delta\phi$ is the phase difference between the two sets of interferometers. The gravity signal can be extracted from the phase shift, and $\Delta\phi$ reflects the gravity gradient.

If there is no noise, a Lissajous curve of the two gravimeters can be obtained and shown as an ellipse. The general algebraic form of an ellipse is

$$F(x,y)=Ax^2+Bxy+Cy^2+Dx+Ey+F=0, \tag{4}$$

where $F(x_i,y_i)$ is called the algebraic distance from point (x_i,y_i) to the ellipse curve. From the ellipse fitting, the phase difference between the two gravity measurements can be expressed as[14]

$$\Delta\phi=\cos^{-1}(-B/2\sqrt{AC}). \tag{5}$$

There is a lot of noise in the atom interference gravity measurement. The Lissajous curve will not appear as a perfect ellipse. As mentioned in the introduction, there are some classic ellipse fitting algorithms. Different algorithms will obtain different gradients. In this paper, we are going to introduce a new algorithm to fit the ellipse. The aim of the algorithm is to minimize the differential-mode noise of the two interference gravimeters and obtain a more accurate value of the gravity gradient. We will also use simulated data to compare the differences in the fitting results of the three different methods.

2.2. The minimum differential noise algorithm

Suppose that the gravimeters are idle instruments, the variation of the sinusoidal signals would only be caused by the gravity, and the amplitude and the offset would not change. ϕ_x and ϕ_y can be written as

$$\phi_x=\phi_0+\phi_{\text{common}}+\phi_{\text{differential}}, \tag{6}$$

$$\phi_y=\phi_0+\Delta\phi+\phi_{\text{common}}-\phi_{\text{differential}}, \tag{7}$$

where ϕ_0 can be referred to as a common mode signal, $\Delta\phi$ can be referred to as a differential mode signal, ϕ_{common} is the common noise, and $\phi_{\text{differential}}$ is the differential noise. The shape of the ellipse is basically decided by the differential mode signal, the common mode signal and common noise will not change the ellipse, and $\phi_{\text{differential}}$ will make the data points discrete.

Referring to Eqs. (2) and (3), we can normalize P_x and P_y to the range $[-1,1]$. We set $P_x=x$ and $P_y=y$, then we can have the following expressions:

$$x'=\frac{P_x-A_x}{B_x}=\frac{x-A_x}{B_x}=\cos\phi_x, \tag{8}$$

$$y'=\frac{P_y-A_y}{B_y}=\frac{y-A_y}{B_y}=\cos\phi_y=\cos(\phi_x+\Delta\phi). \tag{9}$$

Since $\Delta\phi$ is a constant, we can set $c=\cos(\Delta\phi)$, and c can also be expressed as

$$\begin{aligned}c&=\cos(\phi_x-\phi_y)=\cos\phi_x\cos\phi_y+\sin\phi_x\sin\phi_y\\&=x'y'\pm\sqrt{(1-x'^2)(1-y'^2)}.\end{aligned} \tag{10}$$

Then we obtain the elliptic equation after normalizing

$$x'^2+y'^2-2cx'y'-1+c^2=0. \tag{11}$$

Substituting Eqs. (8) and (9) into Eq. (11), we obtain the expression of the ellipse

$$\begin{aligned}&\left(\frac{x-A_x}{B_x}\right)^2+\left(\frac{y-A_y}{B_y}\right)^2\\&-2c\left(\frac{x-A_x}{B_x}\right)\left(\frac{y-A_y}{B_y}\right)-1+c^2=0.\end{aligned} \tag{12}$$

Based on Eqs. (6) and (7), the differential noise of data point (x_i,y_i) is given by

$$\begin{aligned}&|\phi_{\text{differential}}(x_i,y_i)|^2\\&=\frac{1}{2}\left|(\phi_{x_i}-\phi_{y_i})+\Delta\phi\right|^2=\frac{1}{2}\left|\phi_{x_i}-\phi_{y_i}\pm\arccos(c)\right|^2.\end{aligned} \tag{13}$$

The "±" sign is dependent on the value of $\Delta\phi$, but the shape of the ellipse would be the same no mater what the "±" sign

is. Here we choose $\Delta\phi = -\arccos(c)$ and $\Delta\phi > 0$. Then we obtain

$$|\phi_{\text{differential}}(x_i, y_i)|^2 = \frac{1}{2}\left|\phi_{x_i} - \phi_{y_i} - \arccos(c)\right|^2 = \frac{1}{2}\left|\arccos\left(x_i'^2 y_i'^2 \pm \sqrt{(1-x_i'^2)(1-y_i'^2)}\right) - \arccos(c)\right|^2. \tag{14}$$

Since $\Delta\phi > 0$, $\phi_{x_i} - \phi_{y_i}$ would also be positive and close to the value of $\Delta\phi$ when the differential noise is small enough. We believe that the solution which makes the absolute value of $\phi_{\text{differential}}(x_i, y_i)$ minimum would be the solution of the differential noise of the atom interferometer. Then equation (14) becomes

$$|\phi_{\text{differential}}(x_i, y_i)|^2 = \begin{cases} \frac{1}{2}|\phi_+|^2, & \text{when } |\phi_+| < |\phi_-|; \\ \frac{1}{2}|\phi_-|^2, & \text{when } |\phi_+| \geqslant |\phi_-|; \end{cases} \tag{15}$$

where

$$\phi_+ = |\arccos(\sqrt{(1-x_i'^2)(1-y_i'^2)} + x_i'^2 y_i'^2)| - |\arccos(c)|, \tag{16}$$

$$\phi_- = |\arccos(-\sqrt{(1-x_i'^2)(1-y_i'^2)} + x_i'^2 y_i'^2)| - |\arccos(c)|. \tag{17}$$

Let $\boldsymbol{u} = (A_x, B_x, A_y, B_y, c)^{\mathrm{T}}$ be a vector of unknown parameters of the ellipse and consider the nonlinear system of m equations $F(\boldsymbol{u}) = 0$. $F(\boldsymbol{u})$ is given in Eq. (12). Since we obtain the expression of $\phi_{\text{differential}}$, we can use the Levenberg–Marquardt algorithm to minimize the differential noise when $m > 5$:

$$\sum_{i=0}^{m} \phi_{\text{differential}}(\boldsymbol{u})^2 = \min. \tag{18}$$

Since the phase shift reflects the value of gravity, we finally find an algorithm to minimize the differential-mode noise of the two gravimeters. In the following, we will call this method our new minimum differential noise algorithm fitting, which is abbreviated as differential noise fit.

The differential noise fit has many advantages over the traditional methods. Firstly, for the atom interferometer, there is no clear physical meaning for algebraic or geometric distances. The ultimate goal of the algebraic fit or geometric fit is not to obtain the most accurate phase. The differential noise fit is to minimize the differential-mode noise of two interference gravimeters and obtain a more accurate value of the gravity gradient. It is a more direct idea than the algebraic fit or geometric fit.

Another advantage is that the differential noise fit does not have a fitting bias for the differential mode noise. The differential mode noise will cause the ellipse to distort and affect the fitting results. This phenomenon will be illustrated by simulation results in the following. According to the conclusion of Ref. [14] , the algebraic fit and geometric fit will be biased away from the appropriate phase if the data points are noisy. However, if the differential mode noise is randomly distributed, there would be no fitting bias by using the differential noise fit. We will illustrate this with simulation data.

Although there are many advantages, the new method also has disadvantages. One of the disadvantages of the minimum differential noise algorithm is that it cannot handle the normalized data bigger than 1. If $|x_i'|$ or $|y_i'|$ is greater than 1, $\phi_{\text{differential}}$ cannot be solved. If $|x_i'|$ or $|y_i'|$ is close to 1, the solution of $\phi_{\text{differential}}$, according to Eq. (13), would be sensitive to the amplitude noise and the offset noise, while the algebraic fit and geometric fit do not have this problem. We have to sacrifice the data which are bigger than 1 when using the minimum differential noise algorithm to fit the ellipse. In each iteration cycle, we will normalize the data according to the current fitting parameters, and then filter out the data outside the $[-\kappa, \kappa]$ range, where $\kappa \in (0, 1)$. The value of κ can be optimized according to the intensity of amplitude noise and offset noise.

3. Simulation results

This section describes some experiments that illustrate the advantage of our new ellipse fitting method, and its noise performance will be compared to that of some other fitting methods reviewed in the previous section.

The simulation data (x_i, y_i) can be expressed as

$$x_i = A_x + B_x\cos(\phi_0 + \delta\phi_{\mathrm{c}}\cdot\alpha_{\phi_{\mathrm{c}}} + \delta\phi_{\mathrm{d}}\cdot\alpha_{\phi_{\mathrm{d}}}), \tag{19}$$

$$y_i = (A_y + \delta A\cdot\alpha_A) + (B_y + \delta B\cdot\alpha_B) \times \cos(\phi_0 + \Delta\phi + \delta\phi_{\mathrm{c}}\cdot\alpha_{\phi_{\mathrm{c}}} - \delta\phi_{\mathrm{d}}\cdot\alpha_{\phi_{\mathrm{d}}}), \tag{20}$$

$$\phi_0 = \omega\cdot i, \tag{21}$$

where $i = 0, 1, 2, \ldots, 447$, $\omega = 2\pi/28$, the range of ϕ_0 would be $[0, 16\times 2\pi)$, and $\alpha_{\phi_{\mathrm{c}}}$, $\alpha_{\phi_{\mathrm{d}}}$, α_A, α_B are all random numbers $\in [-1, 1]$. We will use three methods to fit the simulation data separately. The first method is the algebraic fit. The second one is geometric distance weighting, which is a modification of the algebraic fit and the solution comes closer to the geometric one.[17] The third one is our differential noise fit. We will use the Levenberg–Marquardt algorithm to solve the fitting problem. We emulate 1000 ellipses, each containing 448 points. The maximum number of iterations of the three methods is 4000, and the tolerance is 10^{-8}.

3.1. Different phase noise fitting results

First of all, we compare the simulation results of the three different fitting methods for different differential noise, while the true value of $\Delta\phi = 0.4$ rad. The amplitude $B_x = 0$ and $B_y = 2$, and the offset $A_x = 1$ and $A_y = 2$. The amplitude noise and offset noise are not included in this simulation, so that δA and δB are zero. The common mode noise $\delta\phi_{\mathrm{c}} = 3$ rad will

not change the shape of the ellipse, but make the data points distributed evenly over the ellipse. The differential mode noise will be set at different values, for example $\delta\phi_{\rm d} = 0.001$, 0.01, 0.1 rad respectively.

Figure 1 shows the simulation data when $\delta\phi_{\rm d} = 0.1$ rad. According to Eq. (1), the phase noise can be converted into gravity noise. If the time interval $T = 60$ ms, and $\delta\phi_{\rm d} = 0.1$ rad, the corresponding gravity noise would be $\delta g = 1.8 \times 10^{-7}$ g. The simulation Lissajous curve will be out of shape and very difficult to distinguish as an ellipse.

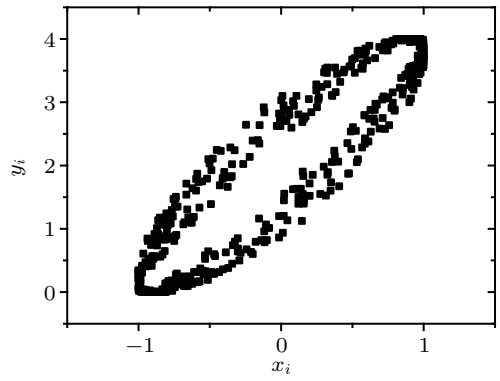


Fig. 1. The Lissajous curve when $\delta\phi_{\rm d} = 0.1$ rad.

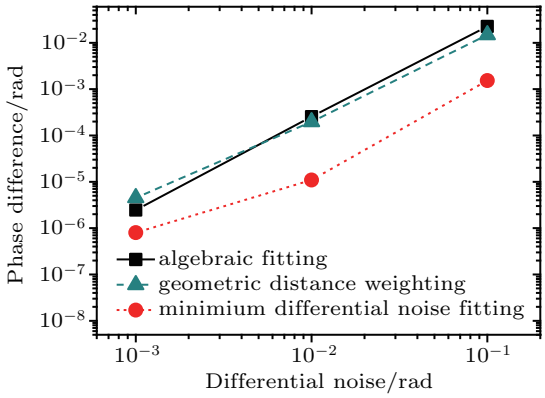


Fig. 2. (color online) The phase difference between the true value and the mean fitting value of three different fitting algorithms under different differential noise.

We calculate the phase difference between the true value and the mean fitting value obtained by the three fitting algorithms, which can be written as $\sum_{i=0}^{N} \frac{\Delta\phi_i}{N} - \Delta\phi$, where $N = 447$, $\Delta\phi = 0.4$ rad, and $\Delta\phi_i$ can be obtained from the fitting results. The comparison of the results is shown in Fig. 2. According to the conclusion of Ref. [14], the algebraic fit and geometric fit results will be biased away from the appropriate phase if the data points are noisy. In theory, the differential noise fit does not have this fitting bias. We find that the differential noise fit obtains the best results, as expected.

Figure 3 shows the standard deviation of the 1000 simulation results for the three different methods. The standard deviation is given by $\sqrt{\sum_{i=0}^{N} \frac{\Delta\phi_i^2}{N} - \left(\sum_{i=0}^{N} \frac{\Delta\phi_i}{N}\right)^2}$. The standard deviation of the differential noise fit is much smaller than the others. When the random noise is small, the fitting standard deviation is proportional to the noise, as demonstrated by the simulation results.

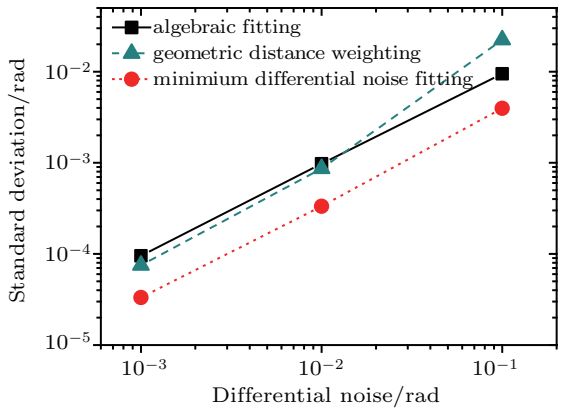


Fig. 3. (color online) The standard deviation of three different fitting algorithms under different differential noise.

We also evaluate the differential noise fit by Allan standard deviation for long term stability in comparison to the traditional methods. Figure 4 shows the Allan standard deviation of three different fitting algorithms when $\delta\phi_{\rm d} = 0.1$ rad. Considering that each ellipse contains 448 points, assuming that the sampling rate of the interferometer is 1 Hz, it takes about 5 days to collect 1000 ellipses. During this time, the Allan deviation result can keep falling.

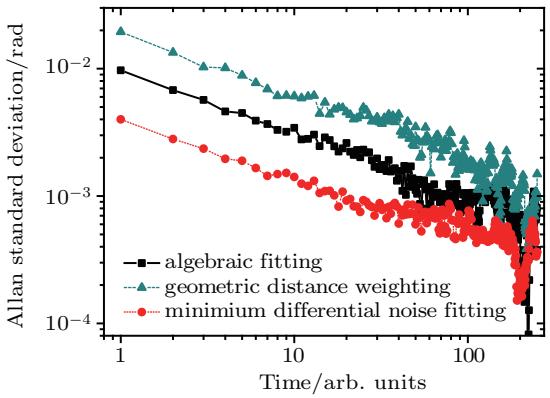


Fig. 4. (color online) The Allan standard deviation of three different fitting algorithms when $\delta\phi_{\rm d} = 0.1$ rad.

3.2. Different phase fitting results

Secondly, we compare the simulated results for different phases $\Delta\phi$ at the same noise level. The differential mode noise $\delta\phi_{\rm d} = 0.02$ rad, and the phase difference $\Delta\phi = 0.2$, 0.3, ..., 1.5 rad. The other parameters are the same as those in the previous simulation.

We compare the standard deviation of the fitting phase for the three methods, as shown in Fig. 5. For all values of $\Delta\phi$, the

differential noise fit obtains the best results. The standard deviation of the differential noise fitting phase can be one order of magnitude smaller than that of the other two methods.

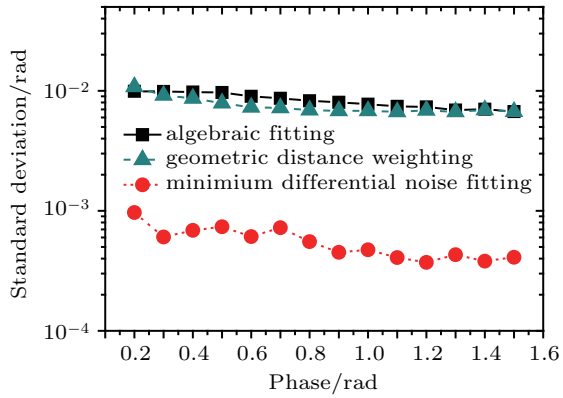


Fig. 5. (color online) The standard deviation of the fitting phase for different $\Delta\phi$.

3.3. Different amplitude noise and offset noise fitting results

In the previous two simulations, differential noise is the only source of noise. The differential noise fit will minimize the differential noise, this is the reason why the differential noise fit can obtain the much better performance than the other two methods. For experiment data, there usually would not be only the phase noise, but also the amplitude noise and the offset noise. We simulate the performance of the three methods in the case with the amplitude noise and the offset noise.

As mentioned in Subsection 2.2, one of the disadvantages of the minimum differential noise algorithm is that it cannot handle normalized data bigger than 1. We set the filter parameter $\kappa = 0.99$ and compare the simulation results for different amplitude noise $\delta B = 0.01, 0.02, \ldots, 0.05$. The offset noise and the differential phase noise are not included in this simulation. The phase difference $\Delta\phi = 0.4$ rad. The other parameters are the same as those in the previous simulation. The simulation results are shown in Fig. 6. The fitting standard deviation is proportional to the noise on the whole. We find that the standard deviation of the minimum differential noise algorithm would be much smaller than that of the other two methods with the increase of the amplitude noise. At $\delta B = 0.01$, there is no big difference between the three methods. But when the amplitude noise is $\delta B = 0.05$, the advantage of the minimum differential noise algorithm is obvious. The standard deviation of the differential noise fit is two times better than the algebraic fit and three times better than the geometric fit. If we optimize the filter parameter $\kappa = 0.90$, the standard deviation would be reduced to 1.387×10^{-5} and still be much smaller than that of the other two methods.

We also compare the simulated results for different offset noise, which is shown in Fig. 7. The offset noise $\delta A = 0.01, 0.02, \ldots, 0.05$. The amplitude noise and the differential phase noise are not included in the simulation. $\kappa = 0.99$ and the other parameters are the same as those in the previous simulation. The standard deviation of the minimum differential noise algorithm fitting can be much smaller than that of the other two methods with the increase of the offset noise. When the offset noise is $\delta A = 0.01$, there is no big difference between the three methods. When the offset noise is $\delta A = 0.05$, the advantages of the minimum differential noise algorithm will be obvious. The standard deviation of the differential noise fit is four times better than the algebraic fit and seven times better than the geometric fit.

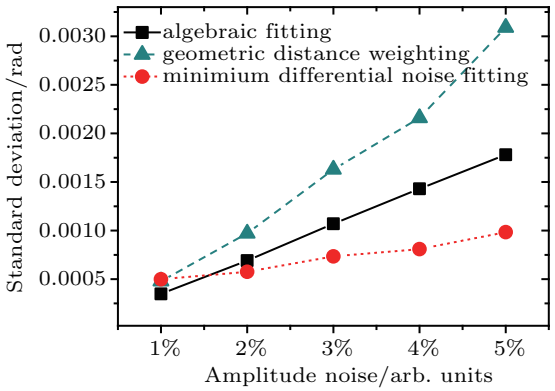


Fig. 6. The standard deviation of the fitting phase for different amplitude noise.

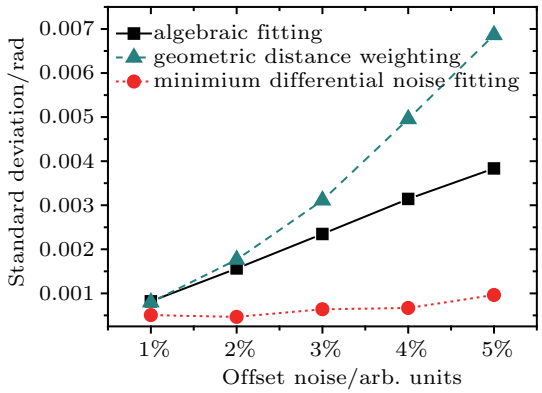


Fig. 7. (color online) The standard deviation of the fitting phase for different offset noise.

4. Conclusion

We have presented a new algorithm to fit the ellipse. We have theoretically derived the expression of the differential mode noise and implemented the ellipse fitting in the program. Our new algorithm is immune to the common mode noise. According to the simulation results, in the cases of different phase noise, amplitude noise, and offset noise, differential noise fitting performs better than algebraic fitting and geometric distance weighting fitting. We also evaluate the differential noise fit by Allan standard deviation for long term stability in comparison to the traditional methods.

In the future, we will explore how to improve the robustness of the algorithm. As discussed in Section 3, the solution

of $\phi_{\text{differential}}$ would be sensitive to the amplitude noise and the offset noise when the normalized data is close to 1. If κ is too large, the filter could not filter out the noisy data. If κ is too small, the fitting data would be too few and could not obtain the good fitting result. The optimization of κ is a way to improve the accuracy of fitting in the actual noise environment. In addition, we have a lot of means to control the phase of the gravimeter in the experiment. By controlling the phase, the normalized data can be prevented from falling beyond $[-1, 1]$, and the robustness of the algorithm may be improved.

The stability of the atom interference gravimeter also needs to be improved. The atom probability is detected by two photodetectors.[23] In the simulation of this paper, we did not introduce the influence of the detection efficiency of the photodetectors. If we want to use the differential noise fit experimentally, the detection efficiency of the two photodetectors must be accurately calibrated, and the atom probability must be normalized. The detection efficiency of the photodetector cannot have significant long-term drift. If these experimental conditions cannot be guaranteed, the differential noise fit may not achieve good fitting results.

References

[1] Sneeuw N, Rummel R and Müller J 1996 *Classical and Quantum Gravity* **13** A113

[2] Tiberi C, Diament M, Caen H L and King T 2001 *Geophysical Journal International* **145** 797

[3] Hu H, Wu K, Shen L, Li G and Wang L J 2012 *Acta Phys. Sin.* **61** 099101 (in Chinese)

[4] Bertoldi A 2006 *Euro. Phys. J. D* **40** 271

[5] Genevès G 2005 *IEEE Trans. Instrum. Meas.* **54** 850

[6] Mashhoon B and Theiss D S 1982 *Phys. Rev. Lett.* **49** 1542

[7] Mashhoon B, Paik H J and Will C M 1989 *Phys. Rev. D* **39** 2825

[8] Paik H J 2008 *General Relativity and Gravitation* **40** 907

[9] Jin W 2015 *Chin. Phys. B* **24** 053702

[10] Wang Q Y, Wang Z Y, Fu Z J and Lin Q 2016 *Chin. Phys. B* **25** 123701

[11] Peters A, Chung K Y and Chu S 2001 *Metrologia* **38** 25

[12] Le Gouët J, Mehlstäubler T E, Kim J, Merlet S, Clairon A, Landragin A and Dos Santos F P 2008 *Appl. Phys. B* **92** 133

[13] Louchet-Chauvet A, Farah T, Bodart Q, Clairon A, Landragin A, Merlet S and Dos Santos F P 2011 *New J. Phys.* **13** 065025

[14] Foster G T, Fixler J B, McGuirk J M and Kasevich M A 2002 *Opt. Lett.* **27** 951

[15] Fixler J B, Foster G T, McGuirk J M and Kasevich M A 2007 *Science* **315** 74

[16] Rosi G, Sorrentino F, Cacciapuoti L, Prevedelli M and Tino G M 2014 *Nature* **510** 518

[17] Gander W, Golub G H and Strebel R 1994 *BIT Numerical Mathematics* **34** 558

[18] Fitzgibbon A, Pilu M and Fisher R B 1999 *IEEE Transactions on Pattern Analysis and Machine Intelligence* **21** 476

[19] Sampson P D 1982 *Computer Graphics and Image Processing* **18** 97

[20] Taubin G 1991 *IEEE Transactions on Pattern Analysis and Machine Intelligence* **13** 1115

[21] Kasevich M and Chu S 1991 *Phys. Rev. Lett.* **67** 181

[22] Wu B, Wang Z, Cheng B, Wang Q, Xu A and Lin Q 2014 *Metrologia* **51** 452

[23] Kasevich M and Chu S 1992 *Appl. Phys. B* **54** 321